

NON-INVASIVE ANALYSIS OF CHEMISTRY IN RYUGU GRAINS BY SYNCHROTRON X-RAY MICROPROBES: PINK-BEAM CT AND TENDER-ENERGY XAS. P. Northrup¹, R. V. Tappero², T. D. Glotch¹, M. Yesiltas³ and Y. Kebukawa⁴, ¹Stony Brook University (Department of Geosciences, Stony Brook NY 11794, paul.northrup@stonybrook.edu), ²National Synchrotron Light Source II, Brookhaven National Laboratory, ³Kirkklareli University, ⁴Yokohama National University.

Introduction: JAXA's Hayabusa2 space mission, which recently retrieved samples from the C-type near-Earth Asteroid 162173 Ryugu, gives us the unprecedented opportunity to study pristine material from a carbonaceous asteroid. Compared to our only other source of such material, meteorites, this material is unaltered by the process of atmospheric entry and exposure on Earth's highly-reactive surface. In order to make the best use of these more pristine samples, and to preserve them for future measurements, we employed non-invasive X-ray techniques requiring virtually no sample preparation or alteration. These techniques specifically probe microscale heterogeneity of elemental distribution and chemical speciation in order to address important questions about the origins of carbonaceous chondritic bodies and subsequent alteration processes that evolved their makeup.

We applied a combination of synchrotron X-ray microprobe pink-beam computed tomography (CT) and tender-energy surface-probing X-ray fluorescence (XRF). Tomography allows us to characterize the interior of the grain without physically cutting sections of it. Tender-energy XRF, although limited to the surface of the grain, provides complementary information about the distribution and chemical speciation of lighter elements such as sulfur. Corresponding microscale X-ray absorption spectroscopy (μ XAS) provides information on chemical speciation, oxidation state, and local structure of selected spots, and can be used to map particular chemical species.

Samples and Methods: Our group was allocated two grains from Ryugu, A0030 and C0034, by JAXA for multimodal analysis [1]. A small fragment of C0034 was mounted for tomography, while the main grain was studied by tender-energy μ XAS and μ XRF.

At the X-ray Fluorescence Microprobe (XFM) at the National Synchrotron Light Source II (NSLSII), pink-beam mode delivers a broad spectrum from about 12 to 22 keV, compound-focused to a $\sim 1 \mu\text{m}$ spot. The advantage of this pink beam is that for transition metals (fluorescence below 12 keV) the background due to scatter is low, while for heavier elements fluorescence is enhanced because the incident beam includes those elements' absorption maxima. A computationally reconstructed fluorescence tomogram consists of one or more virtual "slices" through an

intact particle of appropriate cross-section. The thickness of each slice is defined by the beam size (in this case $\sim 1 \mu\text{m}$), so for the measurements presented here the voxel size is $4 \times 4 \times 1 \mu\text{m}$.

Also at XFM, tender-energy XRF and XAS measurements were made in a helium atmosphere with monochromatic beam energy down to $\sim 2.4 \text{ keV}$. Additional measurements to 2 keV (for phosphorus in particular) can be made at the nearby TES beamline [2]. The lower energy of the incident beam and corresponding fluorescence prohibits measurement more than a few μm below the sample surface, so we measured the surface of the main C0034 grain.

This combination of measurements has particular advantages with respect to 3-D spatial resolution. Conventional hard X-ray microprobe measurements (XRF, XAS, XRD) of prepared thin sections or whole grains will sample the full thickness of the section (typ. $30 \mu\text{m}$) or up to hundreds of μm in a whole grain, so 3-D spatial resolution is defined by sample thickness. Thickness of a tomographic slice is defined by beam size, and for tender-energy measurements the effective sampling depth is comparable to the beam size.

The two data sets can be further correlated by use of light-heavy element proxies. These include Se, which chemically tracks S, and Sr, which can serve as a higher-energy proxy for Ca.

Results: Figures 1 and 2 show two adjacent tomographic slices through the fragment of C0034. Each slice is $\sim 1 \mu\text{m}$ thick, the slices are spaced $10 \mu\text{m}$ apart, and are plotted on the same scale and orientation. Figure 3 shows absorption contrast (z-weighted density) for the slice shown in Figure 2.

Tender-energy measurements of the surface of C0034 show a very heterogeneous distribution of S. Microbeam XAS of several spots showed the presence of both sulfide and sulfate species, as indicated by their respective spectral peaks at around 2471 and 2482 eV. Conducting multi-energy mapping allows us to show the relative distributions of sulfide and sulfate. Figure 4 shows such a map. The majority of S in this sample is sulfide, distributed throughout as fine-grained particles with several large grains, but there are significant discrete spots of sulfate as well. It is important to note that the sulfate and sulfide are independently distributed, rather than showing obvious reaction-rim textures.

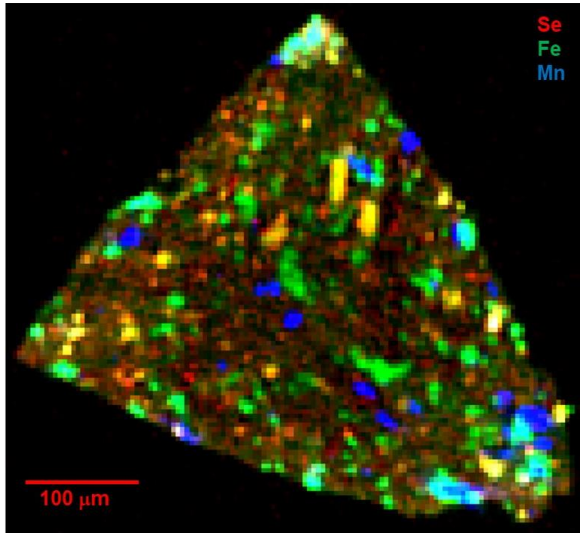


Figure 1. Reconstructed tomographic slice through the fragment of C0034. Image shows 3 elements as red=selenium, green=iron and blue=manganese. Since Se is a chemical proxy for S, orange to yellow spots indicate Fe-rich sulfides, while green spots indicate non-sulfide Fe-rich phases. The distribution of Mn is negatively correlated with Fe and S.

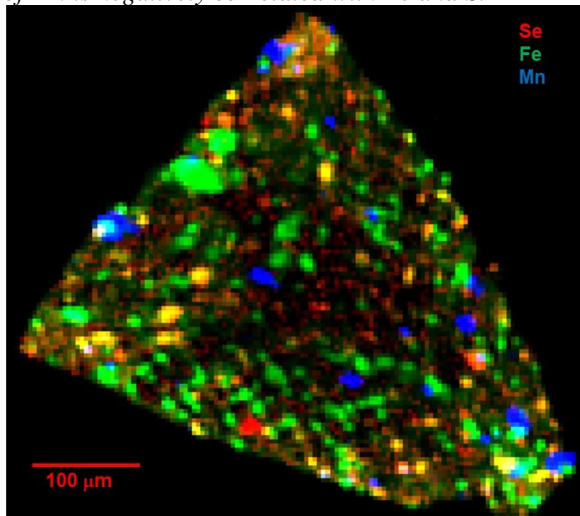


Figure 2. A second tomographic slice through the same fragment of C0034, showing the same 3 elements and colors as Fig. 1. Offset 10 μm from the slice shown in Fig. 1. Note the red spot, a location with high Se (likely S) but low in Fe.

Conclusions: Overall, there is a strong correlation between S and Fe. We observe that Ni, Cr, and Ti are also correlated with Fe, although there are discrete hot spots of Cr and Ti without Fe. A lower concentration of Cr is also broadly distributed across the sample. Cu is sparsely present as individual hot spots, some with Fe and others without. Mn is strongly correlated with Ca, but exhibits a strong negative correlation with Fe

and S. We also observe a few small spots with Zr and a few with Y.

The microscale elemental composition and speciation chemistry has many similarities to carbonaceous chondrite meteorites we have studied [e.g. 3,4], but also some important new observations. The similarities allow us to validate observations made based on meteorite data, while the differences offer us new insights into small body formation and alteration processes.

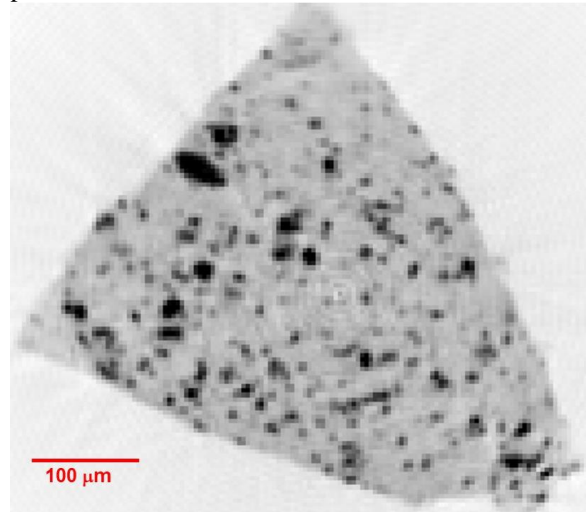


Figure 3. Absorption contrast tomographic slice through the same slice of C0034 as shown in Fig. 2. Darker areas have greater total absorption. Much of the sample is very low absorption.

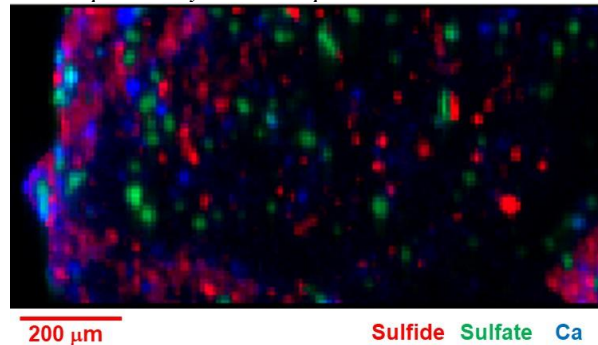


Figure 4. Sulfur speciation map, showing distribution of sulfide (red) and sulfate (green), determined by multi-energy mapping, along with calcium (blue).

Acknowledgments: This work was partly supported under NASA LARS grant 80NSSC19K0940 to P. Northrup. NSLS-II is operated by Brookhaven National Laboratory as a user facility for DOE under Contract DE-SC0012704.

References: [1] Glotch, T. D. et al. (2023), LPSC 54, abstract 2078. [2] Northrup P. (2019) J. Synch. Rad., 26, 2064-2074, [3] Northrup P. et al. (2021) LPSC 52, Abstract 2480, [4] Flores L. et al. (2022) LPSC 53, Abstract 2513.